

CERN-TH/98-277
DESY 98-111
RAL-TR-1998-062
hep-ph/9808433
August 1998

HIGGS RADIATION OFF TOP QUARKS IN e^+e^- COLLISIONS

S. DITTMAIER¹, M. KRÄMER², Y. LIAO^{3,4},

M. SPIRA⁵ AND P.M. ZERWAS⁴

¹ Theory Division, CERN, CH-1211 Geneva 23, Switzerland

² CLRC Rutherford Appleton Laboratory, Chilton, Didcot, OX11 0QX, England

³ Department of Modern Applied Physics, Tsinghua University, Beijing 100084, PR China*

⁴ DESY, Deutsches Elektronen-Synchrotron, D-22603 Hamburg, Germany

⁵ II. Institut für Theoretische Physik[†], Universität Hamburg, D-22761 Hamburg, Germany

Abstract

The strength of the Yukawa coupling of the leptons and quarks with the Higgs boson is uniquely determined by the Higgs mechanism for generating masses in the Standard Model. The top-Higgs coupling can be measured directly in the process $e^+e^- \rightarrow t\bar{t}H$. This process therefore provides a fundamental test of the Higgs mechanism. Extending earlier analyses carried out in the Born approximation, we have determined the cross section for this process including QCD corrections, which turn out to be important.

*Permanent address

[†]Supported by Bundesministerium für Bildung und Forschung (BMBF), Bonn, Germany, under Contract 05 7 HH 92P (5), and by EU Program *Human Capital and Mobility* through Network *Physics at High Energy Colliders* under Contract CHRX-CT93-0357 (DG12 COMA).

1. The masses of the fundamental particles are generated in the Higgs mechanism [1] by interactions with the non-zero Higgs field in the ground state. Within the Standard Model, the Yukawa couplings of the leptons and quarks with the Higgs particle are therefore uniquely determined by the particle masses:

$$g_{ffH} = m_f/v \quad (1)$$

with $v = (\sqrt{2}G_F)^{-1/2} \approx 246$ GeV. The measurement of these couplings provides a fundamental experimental test of the Higgs mechanism *sui generis*.

Several methods have been proposed in the literature to test Yukawa couplings of the Higgs boson [2]. In the present note we focus on the top-Higgs Yukawa coupling. Since the mass of the top quark is maximal within the fermion multiplets of the Standard Model, the ttH coupling ranks among the most interesting predictions of the Higgs mechanism. This coupling can be indirectly tested by measuring the $H\gamma\gamma$ and Hgg couplings, which are mediated by virtual top-quark loops [3, 4]. If the Higgs boson is very heavy, the decay mode $H \rightarrow t\bar{t}$ can be exploited [5]. On the other hand, if the Higgs boson is light, $M_H \sim 100$ – 200 GeV, the radiation of Higgs bosons off top quarks lends itself as a basic mechanism for measuring the ttH coupling. The prospects of operating e^+e^- linear colliders at high luminosities¹ [6] render the radiation process [7, 8]

$$e^+e^- \rightarrow t\bar{t}H \quad (2)$$

a suitable instrument to carry out this measurement.

While for small top masses the top-quark pairs would have been generated at lower energies by photon exchange [7] and the Higgs bosons would have been radiated exclusively off the top quarks, the Z exchange [8] at high energies gives rise to an additional small contribution from Higgs-strahlung. QCD corrections to this process have recently been discussed in Ref. [9], where the Higgs mass has been assumed small with respect to the top-quark mass and the total energy. Rescattering corrections, which are potentially important at non-asymptotic energies, are not properly taken account of by the fragmentation method used in Ref. [9]. In the present analysis we have performed a complete calculation of the QCD radiative corrections to order α_s that is applicable to all kinematical configurations. For high energies, in agreement with the earlier estimates [9], the corrections are negative. At modest energies, however, the corrections are positive and large, and they increase the cross section significantly.

2. The generic set of lowest-order diagrams for the radiation of Higgs bosons off top quarks and Higgs-strahlung in e^+e^- annihilation is shown in Fig. 1a. The QCD corrections can be classified as virtual top-quark self-energy corrections, $tt\gamma$, ttZ and ttH vertex corrections, box rescattering corrections and real-gluon radiation, see Fig. 1b. The

¹In TESLA designs, integrated luminosities of $\int \mathcal{L} = 0.3$ ab⁻¹ and 0.5 ab⁻¹ per year are planned at c.m. energies $\sqrt{s} = 0.5$ TeV and 0.8 TeV, respectively.

total cross section can be split into three parts: the cross section corresponding to Higgs radiation off the top quarks (σ_1, σ_2), Higgs-strahlung off the Z -boson line (σ_3, σ_4), and the interference between these mechanisms (σ_5, σ_6). Each of the contributions has been divided into two parts, generated by the vector couplings of γ and Z to the top pair, and by the axial-vector coupling of the Z . These contributions are different, owing to chirality-breaking mass terms and scalar vertices. In a notation parallel to Ref. [8], but slightly modified, the total cross section may be written in the form

$$\begin{aligned} \sigma(e^+e^- \rightarrow t\bar{t}H(g)) = \\ N_C \frac{\sigma_0}{4\pi} \left\{ \frac{(\hat{v}_e^2 + \hat{a}_e^2)}{(1 - M_Z^2/s)^2} \frac{g_{ttH}^2}{4\pi} (\hat{v}_t^2 \sigma_1 + \hat{a}_t^2 \sigma_2) + \left(Q_e^2 Q_t^2 + \frac{2Q_e Q_t \hat{v}_e \hat{v}_t}{1 - M_Z^2/s} \right) \frac{g_{ttH}^2}{4\pi} \sigma_1 \right. \\ + \frac{(\hat{v}_e^2 + \hat{a}_e^2)}{(1 - M_Z^2/s)^2} \frac{g_{ZZH}^2}{4\pi} (\hat{v}_t^2 \sigma_3 + \hat{a}_t^2 \sigma_4) \\ \left. + \frac{(\hat{v}_e^2 + \hat{a}_e^2)}{(1 - M_Z^2/s)^2} \frac{g_{ttH} g_{ZZH}}{4\pi} (\hat{v}_t^2 \sigma_5 + \hat{a}_t^2 \sigma_6) + \frac{Q_e Q_t \hat{v}_e \hat{v}_t}{1 - M_Z^2/s} \frac{g_{ttH} g_{ZZH}}{4\pi} \sigma_5 \right\}. \quad (3) \end{aligned}$$

The ttH Yukawa coupling g_{ttH} , see Eq. (1), and the ZZH coupling $g_{ZZH} = M_Z/v$ are set off explicitly.² The electric charges are defined as $Q_e = -1$ and $Q_t = +2/3$; $\hat{v}_{e,t}$ and $\hat{a}_{e,t}$ are the vector and axial-vector charges of electron and top quark, normalized as $\hat{v} = (2I_{3L} - 4Qs_W^2)/(4c_W s_W)$ and $\hat{a} = 2I_{3L}/(4c_W s_W)$, with $I_{3L} = \pm 1/2$ being the weak isospin of the left-handed fermions [as usual, $s_W^2 = 1 - c_W^2 = \sin^2 \theta_W = 0.23$]; σ_0 denotes the standard electromagnetic μ -pair cross section, $\sigma_0 = 4\pi\alpha^2/3s$, and $N_C = 3$ is the colour factor of the top quarks. The value of the electromagnetic coupling is taken at $\alpha = 1/128$. The coefficients $\sigma_i (i = 1, \dots, 6)$ can be decomposed into Born contributions σ_i^0 and QCD corrections δ_i :

$$\sigma_i = \sigma_i^0 \left[1 + \frac{\alpha_s}{\pi} \delta_i \right], \quad i = 1, \dots, 6, \quad (4)$$

where we choose $\mu_R^2 = s$ for the renormalization scale³ of the QCD coupling α_s . The total c.m. energy is denoted by \sqrt{s} , and $M_Z = 91.187$ GeV and $M_t = 174$ GeV [10] are the masses of the Z boson and the top quark, respectively.

The QCD radiative corrections have been calculated in the standard way. The Feynman diagrams and the amplitudes for the virtual corrections have been generated with *FeynArts* [11]. They have been evaluated by applying the standard techniques for one-loop calculations, as described in Ref. [12, 13]. Ultraviolet divergences have been consistently regularized in $D = 4 - 2\epsilon$ dimensions, with γ_5 treated naively. Note that the renormalization of the ttH vertex is connected to the renormalization of the top-quark mass, which is defined on shell (see Refs. [4, 13, 14] for details). The algebraic part of the virtual corrections has also been checked by using *FeynCalc* [15]. The infrared divergences encountered in the virtual corrections and in the cross section for real-gluon emission, have

²In the analysis below, v is calculated from the electroweak input data via $v = M_Z c_W s_W / \sqrt{\pi\alpha}$.

³The scale is fixed only to logarithmic accuracy. Different choices of scales can readily be implemented in the definition of the QCD corrections in Eq. (4).

been regularized in two ways, by using dimensional regularization and by introducing an infinitesimal gluon mass; both ways led to identical results after adding the contributions from virtual gluon exchange and real-gluon emission. A second, completely independent calculation of the QCD corrections to the total cross section was based on the evaluation of all relevant cut diagrams of the photon and Z -boson self-energies in two-loop order, generalizing the method applied to $t\bar{t}(g)$ intermediate states in Ref. [16]. The results of the two approaches are in numerical agreement. Finally, we have performed a mutual comparison of partial results with the authors of Ref. [17]; agreement was found between the calculations.

3. The integrated Born coefficients σ_i^0 and the QCD corrections δ_i are too complex to be recorded analytically.⁴ [The corresponding Fortran program is available from DESY [18].] In this letter, we restrict ourselves to the discussion of the basic numerical results for the total cross section. To characterize the relative size of the contributions σ_i^0 , the Born coefficients are shown in Fig. 2a as functions of the Higgs mass for a total energy $\sqrt{s} = 1$ TeV. The corresponding QCD corrections δ_i are shown in Fig. 2b; in the subsequent evaluation of the cross section, the QCD coupling is evaluated at the two-loop level, normalized to $\alpha_s(M_Z^2) = 0.119$ [19].

The size of the QCD corrections is large at modest energies. This is a consequence of the rescattering diagrams, which are generated by the gluon exchange between the final-state top quarks near the $t\bar{t}$ threshold. This Coulomb singularity leads to corrections of the form α_s/β at the $t\bar{t}$ threshold where the top-quark velocity β vanishes in the $t\bar{t}$ rest frame, giving rise to a K factor of the form

$$K_{thr} \rightarrow 1 + \frac{\alpha_s}{\pi} \frac{64}{9} \frac{\pi M_t}{\sqrt{(\sqrt{s} - M_H)^2 - 4M_t^2}}. \quad (5)$$

The pole in β is regularized by the vanishing three-particle phase space for $\beta \rightarrow 0$, when the integration for the total cross section is performed. This effect can be isolated by studying the corrections to the Higgs energy spectrum. For reduced Higgs energies, which shift the $t\bar{t}$ pairs away from the threshold in $t\bar{t}H$ final states, the corrections are gradually reduced. Restricting the Higgs energy to 90% of its kinematically allowed limit, the K factor is reduced from 1.5 to 1.3 for $\sqrt{s} = 500$ GeV and a Higgs mass of $M_H = 120$ GeV. Since the QCD corrections are dominated by the virtual corrections and soft-gluon radiation, the Higgs and top quark energy and angular distributions are hardly changed, leading to a simple rescaling of the Born cross section by an approximately uniform K factor.

At high energies the rescattering corrections become less important, and the positive contributions from gluon emission are overwhelmed by the negative Higgs-vertex corrections, as nicely demonstrated for asymptotic energies in Ref. [9]. For the dominant

⁴The Dalitz densities are given at the Born level analytically in Ref. [8]. Note that the Higgs couplings to fermions g_{ffH} are defined with a minus sign in Ref. [8].

mechanism of Higgs radiation off the top quarks, the reduction of the cross section can be estimated semi-quantitatively in the limit $M_H^2 \ll M_t^2 \ll s$. Since the radiation of a low-mass Higgs boson is in general separated by a large space-time distance from the top production process, the cross section can crudely be estimated by the product of the probability for producing a top-quark pair with the probability for the splitting process $t \rightarrow t + H$. The QCD correction for top-pair production in high-energy e^+e^- annihilation [20] is given by the well-known coefficient $+\alpha_s/\pi$. The QCD correction to the Htt vertex can easily be obtained in the low Higgs-mass limit by the logarithmic mass derivative of the top self-energy [3, 4, 21], leading to $-2\alpha_s/\pi$. Adding up the coefficients $+1 - 2 \times 2 = -3$, these crude estimates suggest a K factor

$$K_{as} \approx 1 - 3 \frac{\alpha_s}{\pi} \quad (6)$$

in the high-energy limit of the Higgs radiation process; *in numeris* the K factor is therefore predicted to be $K \simeq 0.92$ in the TeV range.

Finally, in Fig. 3 we present the cross sections $\sigma(e^+e^- \rightarrow t\bar{t}H + X)$ for three e^+e^- energy values $\sqrt{s} = 500$ GeV, 1 TeV and 2 TeV, as a function of the Higgs mass, in Born approximation and including QCD corrections.⁵ Since the Higgs radiation off the top quarks is by far the dominant subprocess, the cross sections depend approximately quadratically on the $t\bar{t}H$ Yukawa coupling so that the experimental sensitivity to the coupling is very high. This is apparent from Table 1 where the contributions from top-quark radiation (σ_{tt}), Z radiation (σ_{ZZ}), and the interference term (σ_{tZ}) are shown separately. While the phase-space suppression gradually disappears for rising energy, the lower part of the intermediate Higgs mass range is experimentally accessible already at high-luminosity e^+e^- colliders for $\sqrt{s} = 500$ GeV; for $\sqrt{s} = 1$ TeV the entire intermediate Higgs mass range can be covered. For a typical size $\sigma \sim 1$ fb of the cross section for the process $e^+e^- \rightarrow t\bar{t}HX$, about 10^3 events are generated when an integrated luminosity $\int \mathcal{L} \sim 10^3 \text{ fb}^{-1}$ is reached within two to three years of running [6]. This should provide a sufficiently large sample for detailed experimental studies of this process [22].

4. It is straightforward to generalize the present analysis [23]. Within the Standard Model, the calculation of the Higgs energy spectrum and Higgs-top correlations are required experimentally. In the context of supersymmetric extensions of the Standard Model a new calculational element is introduced by the pair production of scalar and pseudoscalar Higgs bosons [8], while mixing effects in the scalar Higgs sector merely increase the complexity of the analysis presented in this note.

Acknowledgements

We thank the authors of Ref. [17] for mutual cross checks of partial results. M.K. and Y.L. are

⁵The K factors are presented in Fig. 4 to simplify experimental simulations of the process.

grateful to Prof. A. Wagner for the warm hospitality extended to them at DESY. We thank W. Beenakker, M. Mühlleitner, and T. Plehn for many helpful discussions.

References

- [1] P.W. Higgs, Phys. Lett. **12** (1964) 132; F. Englert and R. Brout, Phys. Rev. Lett. **13** (1964) 321; G.S. Guralnik, C.R. Hagen and T.W. Kibble, Phys. Rev. Lett. **13** (1964) 585.
- [2] For reviews see: J.F. Gunion, H.E. Haber, G.L. Kane and S. Dawson, *The Higgs Hunters Guide*, Addison-Wesley, Reading, 1990; A. Djouadi, Int. J. Mod. Phys. **A10** (1995) 1; M. Spira, Fortschr. Phys. **46** (1998) 203; M. Spira and P.M. Zerwas, Lectures, 36th Int. Universitätswochen, Schladming, 1997 [hep-ph/9803257].
- [3] J. Ellis, M.K. Gaillard and D.V. Nanopoulos, Nucl. Phys. **B106** (1976) 292; A.I. Vainshtein, M.B. Voloshin, V.I. Zakharov and M.A. Shifman, Sov. J. Nucl. Phys. **30** (1979) 711.
- [4] A. Djouadi, M. Spira and P.M. Zerwas, Phys. Lett. **B264** (1991) 440; S. Dawson, Nucl. Phys. **B359** (1991) 283; D. Graudenz, M. Spira and P.M. Zerwas, Phys. Rev. Lett. **70** (1993) 1372; M. Spira, A. Djouadi, D. Graudenz and P.M. Zerwas, Nucl. Phys. **B453** (1995) 17.
- [5] K. Hagiwara, H. Murayama and I. Watanabe, Nucl. Phys. **B367** (1991) 257.
- [6] E. Accomando et al., Phys. Rep. **299** (1998) 1; *Conceptual Design Report of a 500 GeV e^+e^- Linear Collider*, eds. R. Brinkmann et al. DESY/ECFA 1997-048/182; R. Brinkmann, Report, DESY/ECFA LC Workshop, Orsay, 1998.
- [7] K.J.F. Gaemers and G.J. Gounaris, Phys. Lett. **B77** (1978) 379.
- [8] A. Djouadi, J. Kalinowski and P.M. Zerwas, Mod. Phys. Lett. **A7** (1992) 1765 and Z. Phys. **C54** (1992) 255.
- [9] S. Dawson and L. Reina, Phys. Rev. **D57** (1998) 5851.
- [10] See R. Partridge, CDF/D0, Summary at ICHEP 98, Vancouver, 1998.
- [11] J. Küblbeck, M. Böhm and A. Denner, Comput. Phys. Commun. **60** (1990) 165; H. Eck and J. Küblbeck, *Guide to FeynArts 1.0*, Universität Würzburg, 1992.
- [12] G. 't Hooft and M. Veltman, Nucl. Phys. **B153** (1979) 365; G. Passarino and M. Veltman, Nucl. Phys. **B160** (1979) 151.
- [13] A. Denner, Fortschr. Phys. **41** (1993) 307.
- [14] M. Drees and K. Hikasa, Phys. Lett. **B240** (1990) 455; (E) **B262** (1991) 497.

- [15] R. Mertig, M. Böhm and A. Denner, Comput. Phys. Commun. **64** (1991) 345; R. Mertig, *Guide to FeynCalc 1.0*, Universität Würzburg, 1992.
- [16] A. Djouadi and P. Gambino, Phys. Rev. **D49** (1994) 3499; (E) **D53** (1996) 4111.
- [17] S. Dawson and L. Reina, Preprint, MADPH-98-1073, FSU-HEP-980812, BNL-HET-98/27.
- [18] DESY LC Physics Home Page: <http://www.desy.de/HEP/desy-hep.html>.
- [19] C. Caso et al., Particle Data Group, Eur. Phys. J. **C3** (1998) 1.
- [20] J. Jersak, E. Laermann and P.M. Zerwas, Phys. Rev. **D25** (1982) 1218.
- [21] B.A. Kniehl and M. Spira, Z. Phys. **C69** (1995) 77.
- [22] G. Merino, Report, DESY/ECFA LC Workshop, Lund, 1998.
- [23] S. Dittmaier, M. Krämer, Y. Liao, M. Spira and P.M. Zerwas, in preparation.

\sqrt{s}	M_H [GeV]	σ_{tt} [fb]	σ_{ZZ} [fb]	σ_{tZ} [fb]	σ [fb]	$K = \frac{\sigma_{\text{NLO}}}{\sigma_{\text{LO}}}$
500 GeV	100	1.56	2.97×10^{-3}	1.18×10^{-2}	1.58	1.35
	140	8.85×10^{-2}	8.34×10^{-5}	6.76×10^{-4}	8.93×10^{-2}	2.01
	180	—	—	—	—	—
1 TeV	100	2.47	9.53×10^{-2}	6.15×10^{-2}	2.62	0.95
	140	1.64	8.79×10^{-2}	4.97×10^{-2}	1.78	0.95
	180	1.13	7.88×10^{-2}	3.91×10^{-2}	1.24	0.96
2 TeV	100	7.68×10^{-1}	7.91×10^{-2}	2.72×10^{-2}	8.74×10^{-1}	0.90
	140	5.82×10^{-1}	7.81×10^{-2}	2.57×10^{-2}	6.86×10^{-1}	0.90
	180	4.60×10^{-1}	7.68×10^{-2}	2.41×10^{-2}	5.61×10^{-1}	0.89

Table 1: *The total cross section for the process $e^+e^- \rightarrow t\bar{t}H + X$ including QCD radiative corrections, split into contributions from Higgs radiation off the top quark (σ_{tt}), off the Z boson (σ_{ZZ}), and the interference term (σ_{tZ}), for electroweak parameters as specified in the text. Also shown is the value of the K factor.*

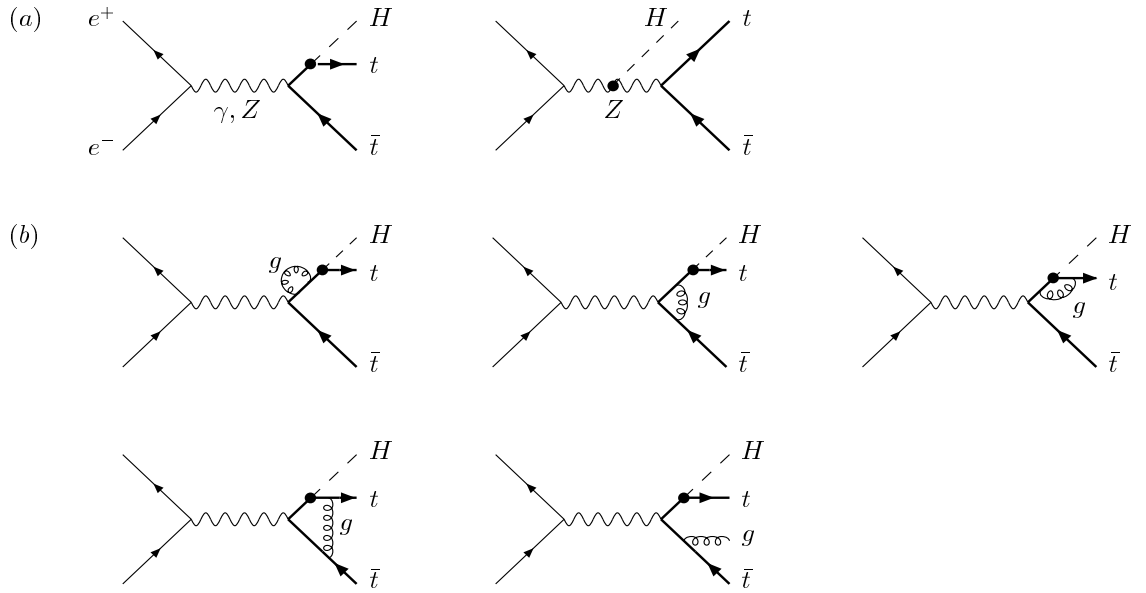


Figure 1: *Generic diagrams contributing to the process $e^+e^- \rightarrow t\bar{t}H(g)$ at (a) lowest and (b) next-to-leading order. The NLO set must be supplemented by the well-known QCD corrections to $Z^* \rightarrow t\bar{t}$, which are not depicted explicitly.*

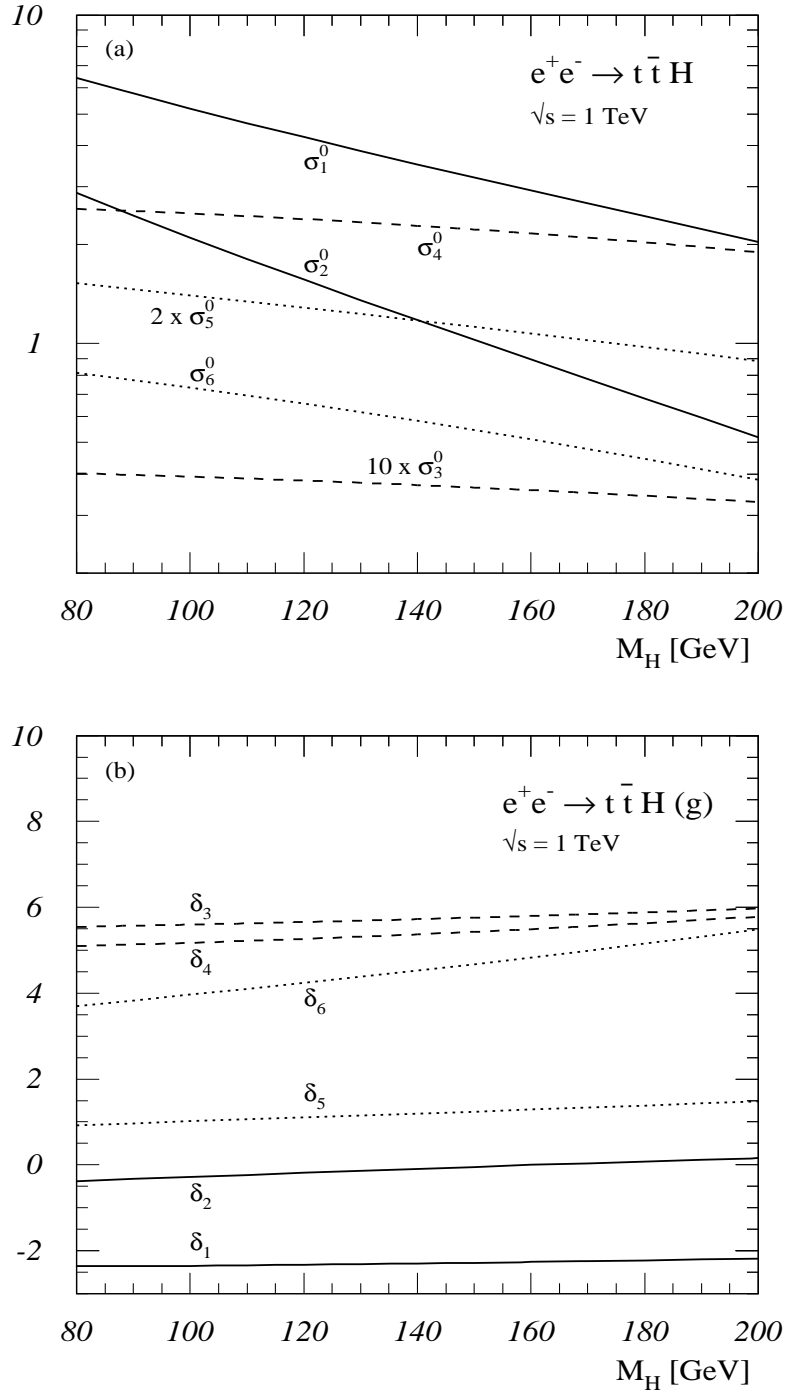


Figure 2: (a) The vector and axial-vector contributions σ_i^0 ($i = 1, \dots, 6$) of Higgs radiation off top quarks, off the Z boson, and the interference term in Born approximation; and (b) the QCD radiative corrections of these terms to order α_s .

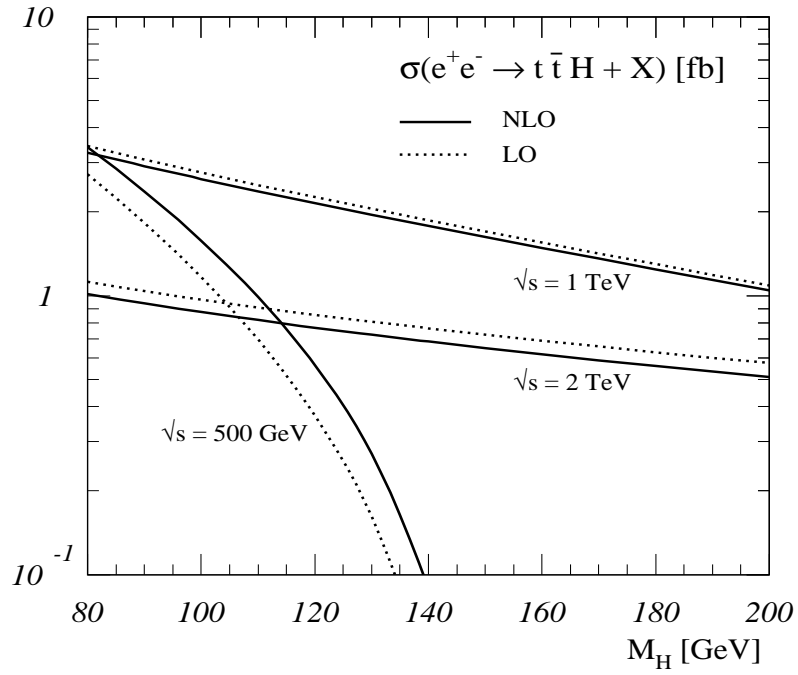


Figure 3: *The total cross section for the process $e^+e^- \rightarrow t\bar{t}H + X$, including QCD radiative corrections, for three collider energies as a function of the Higgs mass (full curves). The Born approximation (dotted curves) is shown for comparison.*

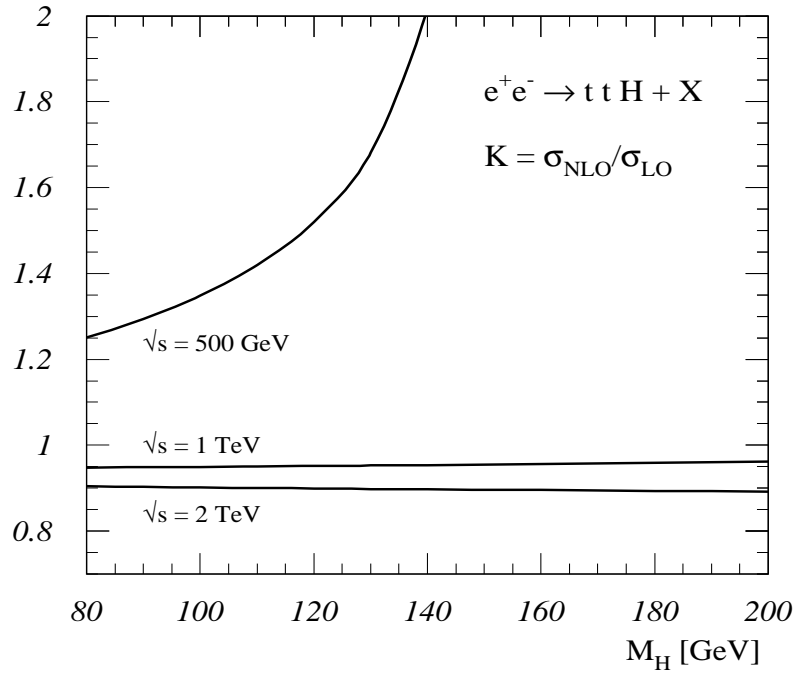


Figure 4: The K factor for the process $e^+e^- \rightarrow t\bar{t}H + X$ for three collider energies as a function of the Higgs mass.

